

Statistical thermodynamics of self-organization of the binding energy super-landscape in the adaptive immune system

József Prechl

R&D Laboratory, Diagnosticum Zrt., Budapest, Hungary

ORCID: 0000-0003-3859-4353

Abstract

The steady flow of energy can arrange matter and information in particular ways in a process we perceive as self-organization. In the case of the humoral adaptive immune system, the steady state of immunological interactions manifests as a self-organized antibody binding energy landscape. Here, I reason that the fusion of energy landscapes creates a super-landscape and the mathematical description of distribution of particle energies can be applied to derive a deformation parameter of thermodynamic potentials in the system. This deformation parameter characterizes the network of interactions in the system and the asymmetry of generalized logistic distributions in immunoassays. Overall, statistical thermodynamics approaches could provide a deeper theoretical insight into the self-organization of the immune system and into the interpretation of experimental results.

Keywords: thermodynamics, self-organization, complexity, systems biology, chemical potential, statistical probability, power law

1. Introduction: self-organization and thermodynamics in the adaptive immune system

Vertebrate animals possess a complex system of cells and molecules that rivals the central nervous system in numerosity and diversity [1]: the adaptive immune system. While the central nervous system adapts the host animal to its macroscopic physical environment, the adaptive immune system controls the molecular environment by maintaining cells and molecules capable of removing their targets. Adjustment of the efficiency of this removal shapes the landscape of targets and maintains molecular integrity of the host [2]. This is what we perceive as protection against infectious agents and tumor cells, as holding the immense microbiota at bay and as the clearance of cellular waste material. Therefore, maintenance of molecular integrity requires the maintenance of constant concentrations of effector molecules, which are called antibodies (Ab) in the case of humoral adaptive immunity. This is achieved by the adjustment of chemical potentials with the help of a sensor-effector feedback mechanism [3], which is the essence of the phenomenon we call immunity. The immune system is dynamic, continuously responding to environmental stimuli, but also shows a tendency to come to “rest”, contract and reach a quiescent state. This resting state can be modeled physically as a steady state [4], a thermodynamically optimized state where minimal effort is required for its maintenance. These features suggest that adaptive immunity is achieved through the self-organization of a complex system (Table 1).

The adaptive immune system evolves with the organism, adapting first (before birth) to a sterile environment comprising only molecules of the host, and later, once exposed to the environment, to the molecules of the outside world. During this process the system learns to bind to target molecular structures, antigens (Ag), in a differentiated manner, tuning the efficiency and quality of target removal so as to maintain molecular integrity of the host. It grows by creating an ordered architecture that bears the imprint of past events: this is immunological memory. Owing to the constant exploration of molecular conformational landscape by cells of the immune system, immunological memory constantly changes, but builds on its past experiences.

Table 1. Cardinal features of self-organization in the adaptive immune system.

Feature	Biological and physical interpretation
Availability of energy	The immune system is part of a living entity, an organism. Cells of the system are bathed in a temperature-controlled environment and are provided nutrients. Long-lived plasma cells are terminally differentiated cells that are metabolically fully devoted to Ab production, while phagocytes efficiently remove Ab-bound antigen. <i>The metabolic energy of cells is used for the biosynthesis of antibody molecules and for the removal of Ab-Ag complexes. Energy essentially appears thermodynamically as μN work: the generation of N particles with μ chemical potential.</i>
Multiple interactions	The blood plasma is crowded with macromolecules: the total protein content approaches that within cells and represents the complete human proteome, with immense diversity and concentration differences. Antibodies themselves further diversify interactions. <i>Humans have about 3 liters of blood plasma with $\sim 100 \mu M$ concentration of Ab molecules, corresponding to about 10^{19} molecules. Common assays use about 10^{-4} liter of serum, roughly equivalent to examining the behavior of 6×10^{14} molecules.</i>
Exploration&exploitation	Antibody molecules are generated by random molecular genetic events, which result in the formation of a structurally highly diverse repertoire. B-cells explore the molecular conformational landscape by their surface Ab and exploit interactions for their survival and clonal expansion. The chemical potential of antigen molecules regulates B cell differentiation by signaling via the B-cell Ag receptor, a membrane-embedded Ab.
Dynamic non-linearity	Feedback mechanisms regulate clonal expansions, adjusting both the availability of interacting molecules and B cells themselves. <i>Dynamic responses to environmental stimuli shape the system, which maintains a steady state. Feedback mechanisms result in a regulated relationship between antibody and antigen thermodynamic potentials.</i>

From a physics point of view, the system is an open one: it is embedded in a thermodynamic reservoir, the host organism, which maintains constant temperature and regulates chemical potentials. It governs the flow of antibody and antigen through the system, adjusts antibody chemical potential and input, thereby controlling antigen levels and output. The system can be driven away from steady state by environmental immunological stimuli. Increased antigen chemical potential is detected by sensor B cells and triggers immunologically controlled responses [5] (Fig.1). These responses can include changing the standard potential (affinity) of antibodies and the change in total free energy (molecule numbers, concentration) of antibodies. Once the chemical potential of the particular antigen is brought to immunologically acceptable levels that cause no harm to the organism, the system contracts. Contraction comprises the death of B cell clones and concomitant selection for survival of those that contribute to thermodynamic steady state maintenance. During both the expansion and contraction phase, chains of

biochemical interactions shape the landscape of chemical potentials as a result of overlapping conformational landscapes [3,6,7].

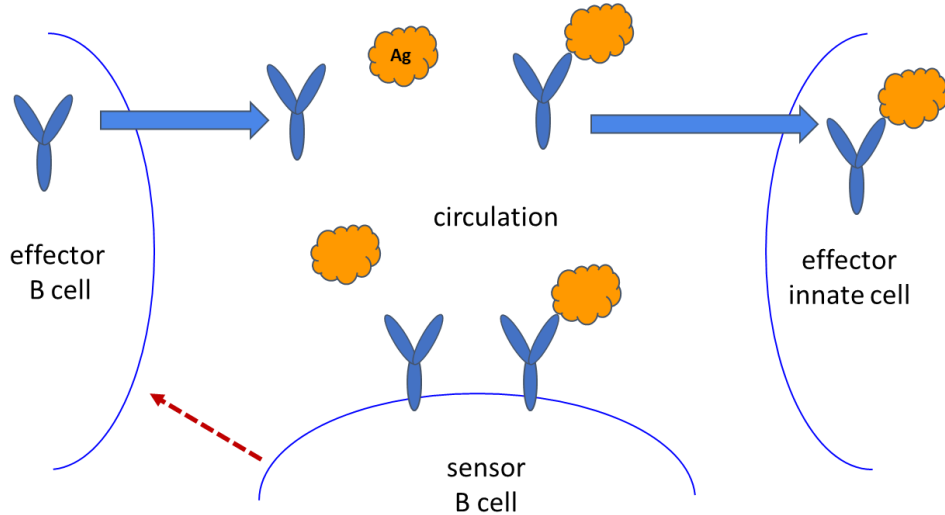


Figure 1. Regulation of Ag levels by self-organization.

Sensor B cells, such as naïve and memory B cells, detect Ag via the engagement of surface Ab and can respond by differentiation (dashed arrow) into effector cells, called plasma cells. Differentiation may involve affinity adjustment besides the secretion of Ab. Ab binds to Ag, generating complexes that are removed by innate effector cells, thereby regulating Ag levels. Blue arrows indicate the flow of Ab that takes along bound Ag molecules.

These events can be monitored by biological techniques that assess the breadth and depth of the immune repertoire on the level of protein sequences [8–13], and various models are used for the analysis and interpretation of the observations [14–18]. Few models exist however that employ universal, statistical physical approaches to the system [19,20]. In the following sections we examine how statistical distributions that are conventionally used in thermodynamics can be applied and interpreted in the description of adaptive immunity and in the analysis of experimental measurements.

2. Energy landscapes of molecules and ensembles

Statistical mechanics and energy landscapes were originally introduced for the modeling of protein folding [21,22]. A funnel shaped energy landscape that guides molecules from conformational diversity towards thermodynamic stability not only helped visualize entropy-energy compensation in the process of folding but generated answers about the thermodynamics, kinetics and evolution of macromolecules and their interactions [23–29]. It turns out that binding mechanisms, where intermolecular rather than intramolecular interactions operate, can also be explained by funnel energy landscapes of folding and binding [23] and free energy landscapes in general [30,31]. It is therefore reasonable to apply this model to a biological system, which regulates extracellular molecular interactions: humoral immunity – primarily but not exclusively – adjusts the concentrations of target molecules, antigens, via the directed evolution of a system of antigen binding proteins, the antibodies.

Here, we assume that self-organization drives the system of antigen and antibody molecules towards a steady state, which encompasses the fusion of binding energy landscapes of individual antigens and antibodies, generating a super-landscape (Fig.2). We regard the totality of interacting antigen and antibody molecules as an ensemble of conformational isomers, with conformational diversity originating from sequence differences (molecular diversity) and structural dynamism (conformer diversity). The entropy of the physical system thus has two origins: 1, molecular diversity, where gene and protein sequence differences lead to distinct structures; 2, folding diversity, where the same molecule or complex can attain distinct structures (conformational isomers) via allosteric dynamism. Molecular diversity is a property of the system, while folding diversity is the property of an individual

molecule. This distinction is important because organization is mediated by cells and the genetic content of cells determines clonality and thereby molecular diversity. In our model we assume that a strict entropy-energy compensation mechanism governs events, in the sense that entropy of the non-native states (funnel top area) determines energy of the native state (funnel depth) and vice versa, a certain native state energy directly implies a given non-native entropy (Fig.3).

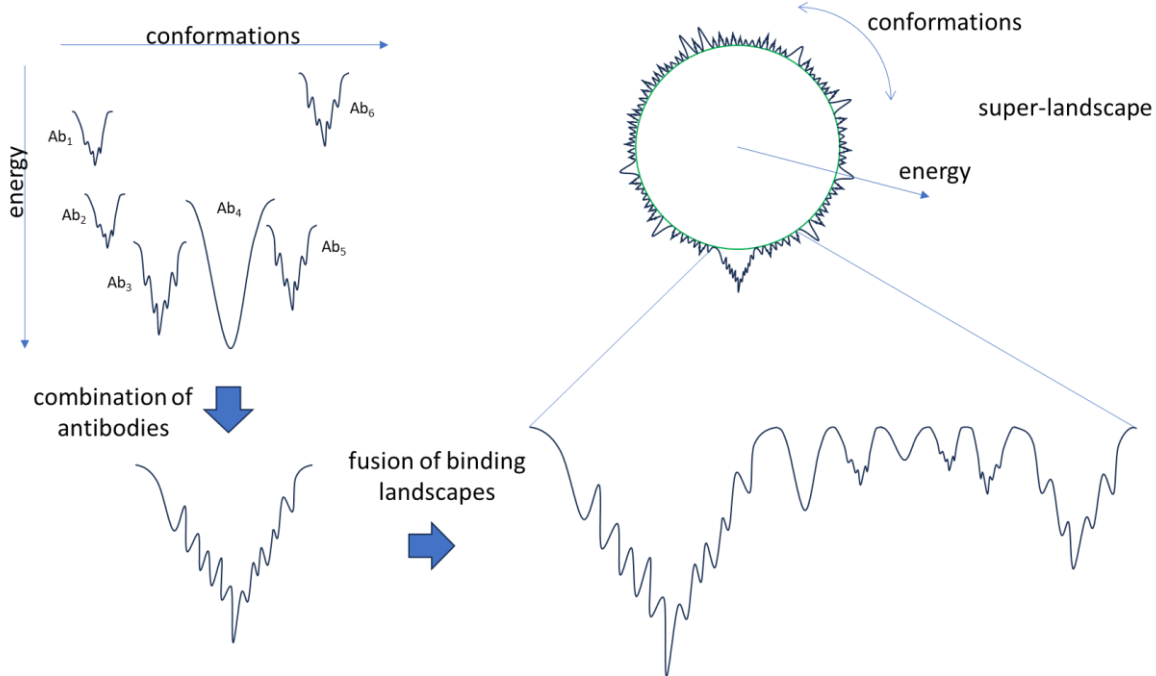


Figure 2. Binding energy landscapes. Antibody clones shape the binding energy landscape of antigen; the totality of antibody clones and antigen molecules creates a global super-landscape.

The contraction of an immune response following the active clonal expansion phase corresponds to the process of fusion of energy landscapes of newly generated antibody clones and of newly adjusted antigen targets. From the biological point of view this process selects antibody clones that fit into the already established immunological memory and adjusts antigen concentration. From the physical point of view this process is the compensation of binding energy and entropy. That antibody conformational isomerism can contribute to diversity [32,33] and is modulated by antibody maturation [34] has long been recognized. While individual antibodies have been treated as conformational ensembles of the binding site [35], and the antigen binding fragment [36,37], the modeling of the complete repertoire as an ensemble of fused binding energy landscapes of dynamic conformational ensembles holds the promise of a physical model of the humoral immune system. Landscapes of antibody-antigen interactions have been used to characterize immunity [38–40].

The free energy of binding is given by the equation [27,41,42]

$$\Delta G = E_N + \frac{1}{\beta} \ln \left[\sum_{E>E_N} g(E) e^{-\beta E} \right] \quad (1)$$

where ΔG is free energy difference, E_N is the ground-state energy of the native structure, β is thermodynamic $\beta=1/kT$ (k is Boltzmann constant, T is thermodynamic temperature), $g(E)$ is the density of states, E is energy level. We can simplify the above expression by using natural units of energy, nat, so we will be omitting β from the formulae here on. This expression assumes there is only a single unique native structure, in which case the difference in energy between the native state and the sum of energies of non-native states determines free energy change of binding.

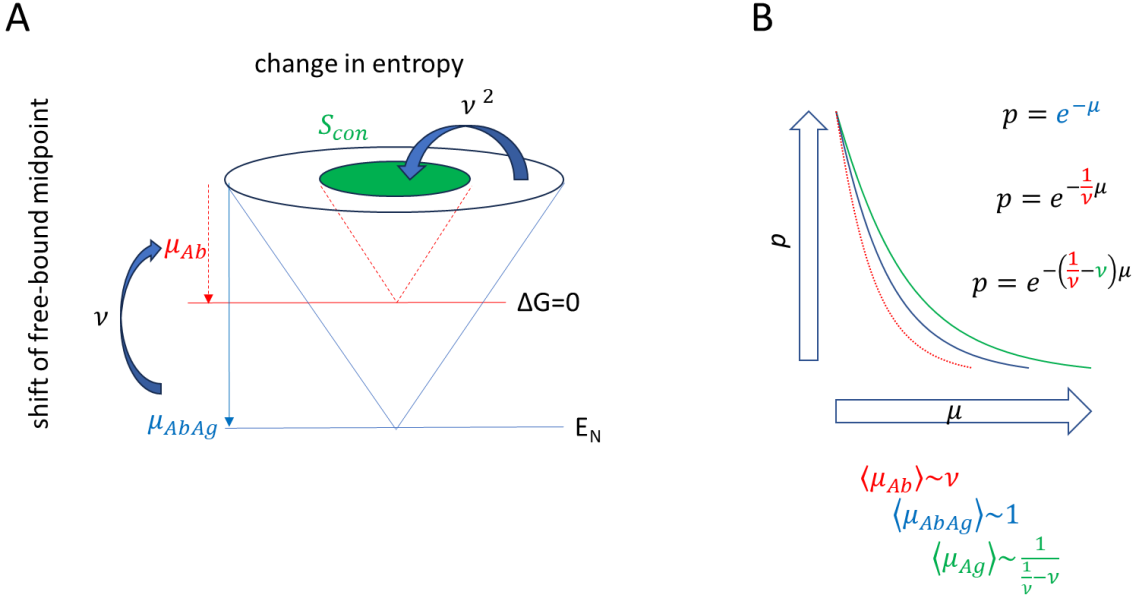


Figure 3. Distribution of chemical potentials of the binding landscape.

The free-bound midpoint in the energy funnel characterizes the free energy of Ag molecules (A), which drives Ag towards the bottom of the funnel. The conformational entropy corresponding to that fraction of the funnel is proportional to the square of the factor of energy ratios. Exponential distributions of chemical potentials of free Ab (red), bound Ab (blue) and free Ag (green) are determined by the proportionality factor ν .

The energy level of the free-bound midpoint, where $\Delta G=0$, is determined by the density of states, which in turn is determined by the affinity and availability of antibodies creating the binding funnel. The antibody binding affinity landscape combines with the energy landscape of antigen resulting in a perturbed free energy landscape [31], which determines this value. Immunological mechanisms can adjust both funnel depth by tuning affinity and chemical potential by adding and removing molecules and their complexes to and from the system (Fig.1). Excess antigen drives antibody maturation with increased affinity, while excess antibody deprives B cells from survival signals by removing antigen. Self-organization can therefore be described as the shaping of the antigen energy landscape: moving antigen molecules deemed dangerous by the immune system to deeper funnels with increasing stability of their bound forms.

3. From equilibrium to steady-state molecular ensembles

The Boltzmann distribution describes the distribution of distinguishable, non-interacting particles in thermal equilibrium with an infinite reservoir, with probability p

$$p \propto \frac{1}{e^E} \quad (2)$$

where E is energy of the particle. This proportionality results in an exponential distribution that maximizes entropy of the system of particles for a given mean energy.

In our model we assume that antigen energy is exponentially distributed, based on experimental and theoretical reasons. Models of fluctuating antigenic landscape [43] and experimental determination of clone sizes [44] revealed that lymphocyte clone sizes follow power law. Power law distribution is generated when deterministic exponential growth is stopped at random time, which is exponentially distributed [45]. It follows that if antigen stimulus induces exponential growth of lymphocytes and is stopped at exponentially distributed time intervals clone size is distributed according to power law.

Antigen stimulation for exponentially distributed time intervals corresponds to an exponential distribution of antigen energies.

Using the funnel energy landscape model, we can relate free energy change to the maximal free energy change (corresponding to the native state energy) by introducing a factor, ν , and chemical potentials

$$\nu = \frac{\Delta G}{E_N} = \frac{\mu_{Ab}}{\mu_{AbAg}} \quad (3)$$

where μ_{Ab} is the chemical potential of free Ab and μ_{AbAg} is the chemical potential of the bound Ab.

Let us now consider a system with a Boltzmann distribution of chemical potentials of distinguishable molecular entities. Let the states be distinguishable by vector directions in a configuration space, where directions correspond to molecular structures (conformations) and thereby binding specificities [7]. The system of molecules can also be characterized by their conformational entropy, their potential to explore the conformational space in search of interaction partners, orthogonally to the vector direction. In a steady state, the chemical potentials of the molecule species are distributed (Fig.3B) according to

$$p \propto \frac{1}{e^{\frac{1}{\nu} \mu_{Ab}}} = \left(\frac{1}{e^{\mu_{Ab}}} \right)^{\frac{1}{\nu}} \quad (4)$$

Global interactions modify the distribution of chemical potentials and this is represented by the exponent $\frac{1}{\nu}$. Interaction here means an overlap of the conformational landscapes explored by the interacting molecules, the extent of cross-reactivity of Abs. Thus, it is not a direct molecular binding but an effect on the availability of molecular targets and an effect on the chemical potential. These interactions, the global fusion of binding landscapes modifies the average chemical potential in the system by the factor ν . Thus, compared to the special case, when $1/\nu$ equals 1, the average chemical potential of Ab decreases. Here ν is a deformation factor for the average extent of interactions in the system. Eq.(4) also reveals that ν has a modulating effect on thermodynamic β or inverse temperature $1/T$, which can be interpreted as increasing $1/\nu$ corresponding to enriching the conformational space at a given temperature.

Thus, ν expresses the change of density of states in the system due to interactions, the extent of fusion of energy funnels in the super-landscape. It is important to note that ν is an average value for the whole system while sampling of the system estimates the value of local subnetworks and may give different values from this global average (see later).

Ideal binding for all the components of the system, considering a strict entropy-energy compensation, would require that all the non-native conformers of the antigen molecules are thermodynamically driven to the native state. This driving force can be represented by the conformer entropy and the decrease in binding free energy change can also be expressed in terms of entropy, which – being an area – changes by the square of the deformation factor

$$S_{con} = \nu^2 E_N = \nu^2 \mu_{AbAg} = \nu \mu_{Ab} \quad (5)$$

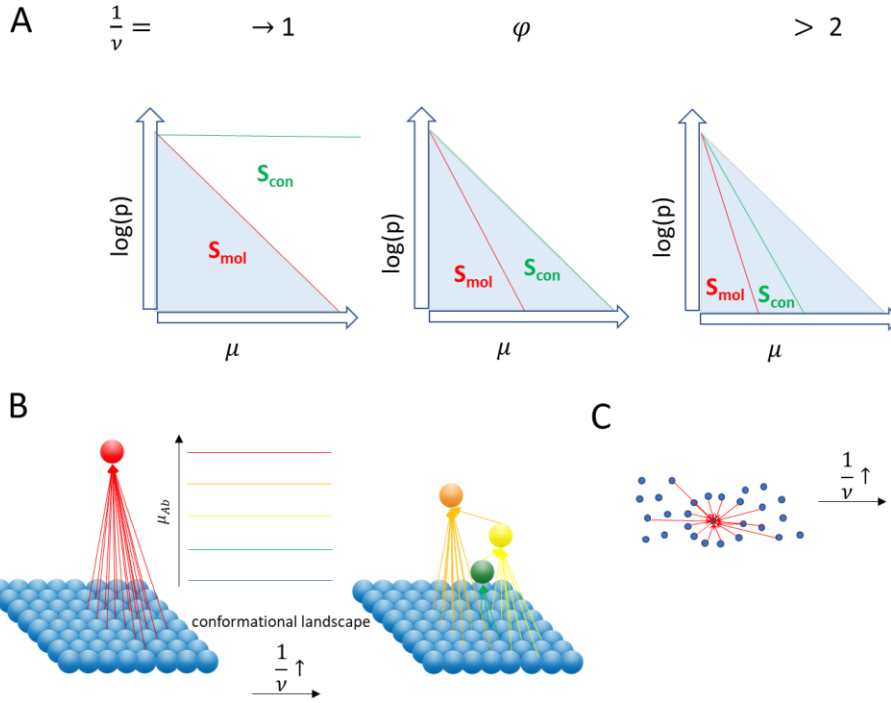


Figure 4. Effect of ν on molecular and conformational entropy, energy levels, and network topology. Shaded areas represent the potential associated with the binding funnels, S_{mol} is molecular entropy, S_{con} is conformational entropy (A). The chemical potential hierarchy of network nodes of Ab (B) determines the flow of Ag toward higher affinity interactions (red arrows), and are characterized by the deformation parameter (C).

We can combine Eq. (4) and (5) by introducing the later as a degeneracy factor. The generation of multiple bound forms of the antigen molecule contributes to degeneracy: states with identical energy level. The higher the concentration of Ab, the greater the driving force for binding, and the higher is the degeneracy in the system. This entropic force appears as an excess Gibbs energy of Ag, so we can express the chemical potential distribution of Ag as a function of Ab chemical potentials

$$p(\mu_{\text{Ag}}) \propto (e^{\mu_{\text{Ab}}})^{\nu} \left(\frac{1}{e^{\mu_{\text{Ab}}}} \right)^{\frac{1}{\nu}} = e^{-\left(\frac{1}{\nu} - \nu\right)\mu_{\text{Ab}}} = \left(\frac{1}{e^{\mu_{\text{Ab}}}} \right)^{\left(\frac{1}{\nu} - \nu\right)} \quad (6)$$

where μ_{Ag} is the chemical potential of Ag interacting with Ab with probability $p(\mu_{\text{Ag}})$. The higher the overlap between binding funnels in the fused binding energy landscape ($\nu \downarrow$), the less conformational entropy needs to be reserved per Ag species, and the greater the molecular diversity becomes with a total given number of molecules, but at the expense of specificity. At the extreme, interactions become random (Fig. 4C, right diagram).

If the value of ν approaches 1, the exponent in Eq. (6) approaches 0 and the mean energy of the system goes to infinity. This is equivalent to stating that it would require an infinite concentration of Ab to reach the complete saturation of all Ag and to drive all Ag molecules to the bottom of the binding funnel. In other words, it is impossible to maintain a system with a huge number of diverse molecules and reserve completely isolated binding energy landscapes, preventing their fusion. As ν decreases ($\nu < 1$) it reaches a point where $\frac{1}{\nu} - \nu$ equals 1 and the $p(\mu_{\text{Ag}})$ function reduces to

$$p(\mu_{\text{Ag}}) \propto e^{-\left(\varphi - \frac{1}{\varphi}\right)\mu_{\text{Ab}}} = e^{-\mu_{\text{Ab}}} = \frac{1}{e^{\mu_{\text{Ab}}}} \quad (7)$$

where φ is the golden ratio, numerically $(1+5^{1/2})/2$. In this ideal state, enthalpy-entropy compensation in the interaction space leads to a steady state, where the expected value of Ag chemical potentials is equal to that of the AbAg complexes (Fig.3B).

Thus, ν has a unique value that indicates ideal, quasi-equilibrium state in the system.

4. From chemical potential to thermodynamic activity: networks with power law

Exponential distributions correspond to power law distributions via the following mathematical relationship. If P is the complementary cumulative distribution function (cCDF) of μ_{Ab}

$$P(M_{Ab} > \mu_{Ab}) = e^{-\frac{1}{\nu}\mu_{Ab}} = (e^{\mu_{Ab}})^{-\frac{1}{\nu}} \quad (8)$$

in the sense that a randomly sampled chemical potential M is greater than μ with probability P , and μ is distributed exponentially with scale parameter ν , then the absolute thermodynamic activity $\lambda = e^\mu$ will have a cCDF following power law as

$$P(\Lambda_{Ab} > \lambda_{Ab}) = \lambda_{Ab}^{-\frac{1}{\nu}} = (e^{\mu_{Ab}})^{-\frac{1}{\nu}} = (e^{\mu_{Ab}})^{-\frac{1}{\nu}} \quad (9)$$

This suggests that the value of ν determines the organization of a thermodynamic network of interactions: it is the exponent of the power law distribution of network node degrees, which represent molecules with a given thermodynamic activity. Thermodynamic activity describes the probability of interacting with another molecule and thereby here it corresponds to the degree of the node representing the molecule in the interaction network of fused binding energy landscapes.

It has long been recognized that fractals possess thermodynamic properties and fractal characteristics are analogous to statistical mechanics variables [46]. If fractal systems have an entropy [47], then a thermodynamic system with fractal properties can be characterized by its fractal dimension. In a geometric fractal the number of measured parts N is related to the measure size E by a power law relationship with exponent D , the fractal dimension and K is measured part when $E=1$

$$\frac{N(E)}{K} = E^{-D} \quad (10)$$

In our system fractality is interpreted as the number of molecules with thermodynamic activity E distributed according to power law with exponent D . Whereas in a geometric fractal the increasing resolution (decreasing E) reveals more details behind coarse structures, more N parts, in our system increasing resolution means counting molecules with smaller thermodynamic activity λ , revealing more and more molecules “behind” network hubs [48,49]. Unlike for a geometric fractal object, in our system the total number of components is proportional to the area under the curve of cCDF. The value of $1/\nu$ as fractal dimension is an index of the complexity in the pattern of interactions in the system (Fig.1D).

Thus, ν characterizes the power law distribution of probability of interactions in a system with fractal network properties.

5. Probing the system: equilibrium titration

The Fermi-Dirac distribution (FD) describes the occupancy of energy states by indistinguishable particles

$$p(E) = \frac{1}{1+e^{(E-\mu^0)}} \quad (11)$$

where μ^0 is the energy of the state where half of the states are occupied (Fermi energy), E is energy of particle and again we assume $\beta=1$ for simplicity (Fig. 3). From the mathematical point of view, FD is

the complementary distribution of the logistic distribution (LD) (see Appendix A), which is used for modeling equilibrium titration of biochemical reactions with a parametrization similar to that of FD

$$p = \frac{1}{1+e^{-(\mu-\mu^0)}} \quad (12)$$

where μ^0 is the average energy of the reaction, and p is probability of completion of reaction when μ probe (interaction partner) potential is applied. Of note, completion of reaction means that all molecules have engaged with the titrating interaction partner: they have all been probed. This family of functions is in use in several fields of science and is also referred to as four-parameter logistic function or 4PL for immunoassays [50,51], Hill-equation for ligand binding assays [52–54], and Langmuir-equation for surface adsorption [55]. From the information theory point of view these functions are used for calibrated binary classification problems [56]: in the case of fermion particles binary classification means the occupation or emptiness of a particular energy state as a function of energy, while for biochemical reactions it gives the probability of bound versus unbound state as chemical potential is changed (Fig. 5A,B). Even population growth can be interpreted as an energy function: with the passage of time the growing entity uses up its resources, meanwhile the available energy decreasing gradually (see Appendix B). Thus, the complementarity between the Fermi-Dirac and logistic distributions is not simply mathematical: if the first is the probability of occupancy energy states, then the second is the distribution of emptiness of energy states in the same system (Fig. 5), in the sense that it shows how energy states are filled up upon probing.

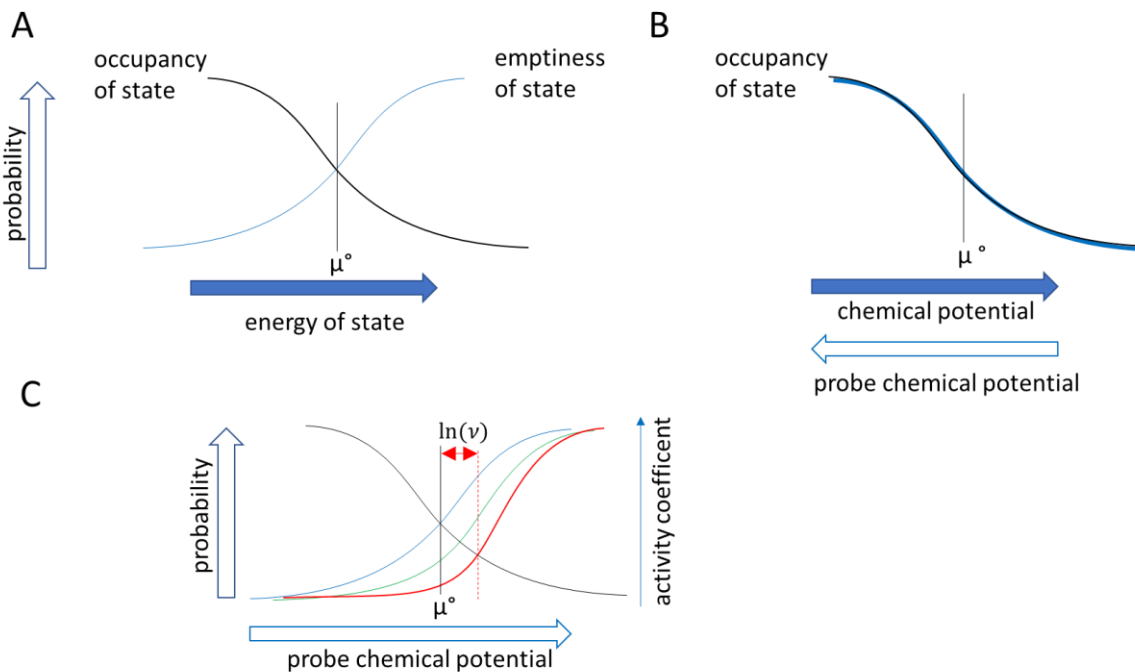


Figure 5. The Fermi-Dirac (black line) and the logistic (blue line) distributions are complementary (A). The chemical potentials of probed (black) and probing (blue) molecules have opposite signs (B). Relationship of distribution of chemical potentials of antibodies and that of the probing antigen as modeled by a generalized logistic function(C), where ν determines deformation (green and red lines). μ^0 represents standard chemical potential.

If the FD distribution gives the probability of being unbound, at a relative distance from mean energy, then the LD gives the probability of being bound. In equilibrium titration assays mean energy corresponds to the logarithm of equilibrium dissociation constant K_D , and energy corresponds to the chemical potential or logarithm of concentration. Since equilibrium is established, the two components (system and probe molecules) have opposite signs for their potentials (Fig. 5B). Probing the system that

comprises distinguishable molecules renders the molecules indistinguishable: they are all identical in the sense of binding to the probe, the difference between them being the free energy of binding. The Pauli exclusion principle here means that any antigen binding site can be occupied by one Ab molecule only. Probing the system means the measurement of local distance of chemical potential from the system average potential, $\mu - \mu^0$. Beyond this distance the probe is more likely to be empty, within this distance the probe is more likely to be occupied. A measurement method that probes a system by equilibrium titration essentially fits a logistic distribution to the measurement, implying that the observed cumulative distribution is the result of the underlying Fermi-Dirac distribution of particle energy states. In the case of antibody-antigen interactions such a titration reflects the free energy distribution of the interacting molecules, and is the sum of Gibbs and excess Gibbs energies.

Whereas the logistic function describes ideal binding and growth curves, real-life data often poorly fit such curves. The reason is that there are different kinds of interactions between the probed molecules and/or the probe molecules themselves. These are better fitted by generalized logistic or other growth functions [57]. It is also important to use an appropriate probing method, which is capable of detecting deformations in the binding curve without altering properties of the system [58–60]. A surface covered by Ag molecules is a chemical probe with a chemical force defined by the density of Ag. This chemical force is the chemical potential of the Ag probe. By increasing the density, we can exert increasing chemical force on the system, probing “deeper” into the system. On the molecular levels this means that components of the system that are less specific/less affine for the molecular Ag probe will gradually start to bind to the probe. This is registered by the increasing density of bound antibody and the increasing proportion of bound Ag. The rate of increase at any point is determined by the antibody composition of the system, and this composition is reflected by the slope of the binding curve. A homogenous system will present as a symmetric binding curve. A heterogenous system, on the other hand, will present as an asymmetric binding curve [50]. In the statistical mechanics interpretation, the particles influence each other’s probabilities, interact. From the immunochemical point of view, antibodies compete (cross-react) with each other.

If heterogeneity means the number of distinct molecules contributing to a chemical potential vector, we can again use the deformation parameter factor that represented change of chemical potential with respect to change of free entropy, now applied to a subset Ag of configuration space, expressed as ν_{Ag} . This subset is the collection of interactions with the probing antigen, the fraction of the conformational space representing epitopes of the probing antigen. The chemical force exerted by a heterogenous antibody solution on the probe is modeled by the generalized logistic distribution (Fig. 5C)

$$p = \left(\frac{1}{1 + \nu e^{-(\mu - \mu^0)}} \right)^{\frac{1}{\nu}} \quad (13)$$

which we use with the parametrization of Richards [61][62][60] so as to keep the meaning of μ^0 as the value at point of inflection.

Based on the deductions above, the asymmetry parameter ν_{Ag} has a physico-chemical and a statistical thermodynamics interpretation. In the case of a homogenous system, such as a monoclonal antibody, the distribution is symmetric, the asymmetry parameter has a value of 1 and the function reduces to the logistic distribution. In the case of non-interacting molecules their energy levels are described by the cCDF of the logistic distribution. For interacting particles, such as cross-reactive antibodies, the asymmetry parameter characterizes the extent of interaction in terms of proportions of extensive conformational entropy to extensive molecular entropy (Fig.3A), where a value of 1 means no interaction and decreasing values mean increasing interaction. From the physico-chemical point of view, the asymmetry parameter is related to the limiting activity coefficient or activity coefficient at infinite dilution [63]. It is important to note that the value of ν for the system is the average of all local ν values and can differ from local measures of ν_{Ag} obtained by probing the system. The more specific and

localized in configuration space e.g. a single epitope) the probe is, the more v_{Ag} can differ from the system average.

Thus, v_{Ag} characterizes deformation of distribution of interactions locally, with respect to a specific Ag component of the system, in an experimental measurement technique.

6. Discussion

In this paper the statistical properties of a complex system are described as a physical ensemble in a biological organism. The biological purpose of this system is the maintenance of molecular integrity of the organism. Physically that is interpreted as the maintenance of a steady state of interactions between entities of the system, Ab and its targets, Ag. While the system is highly dynamic, its resting state can be modeled by a steady state wherein the chemical potentials of the molecular components are adjusted so as to drive the system towards quasi-equilibrium. With the assumption of a tendency to reach steady state we also assume that canonical functions of statistical thermodynamics are applicable to the system. Analogues of the Boltzmann and the Fermi-Dirac distributions, which are used to define particle energies, appear in the functions herein used for molecular components of the adaptive immune system. What we intend to highlight in this paper is that the organization of interactions between components of the self-organizing system is captured by a variable, here denoted by v , which reflects a deformation in the system (Fig. 6). This variable determines the distribution of chemical potentials, the network of interactions and the binding curves obtained by experimental probing of the system.

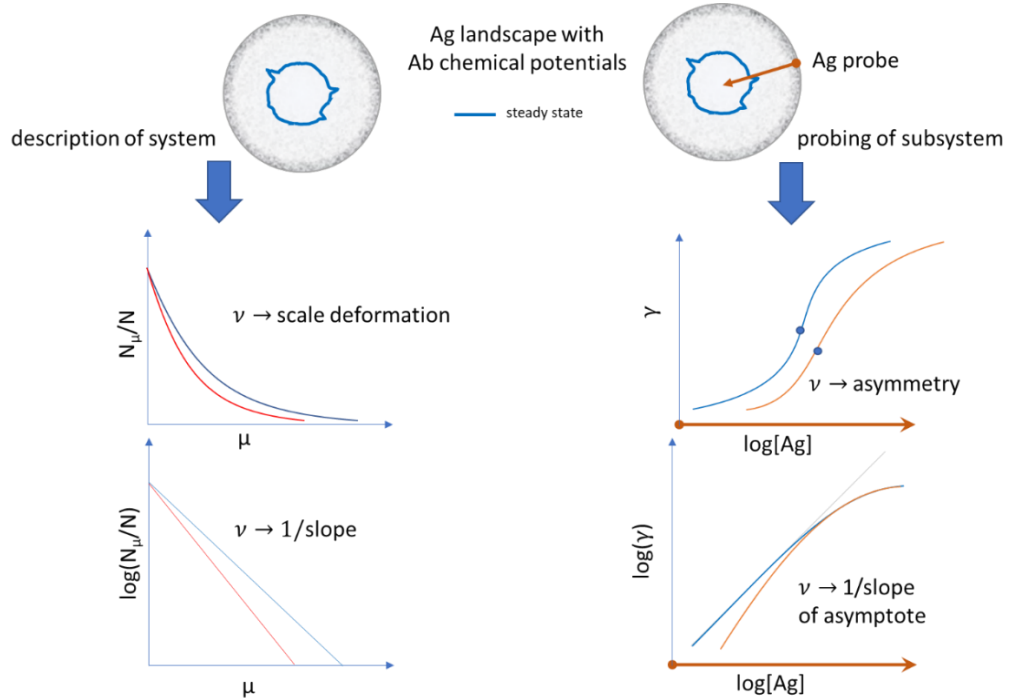


Figure 6. The deformation parameter v defines statistical distributions of the complete system and of the probed subsystem. The value of v determines the scale, slope, asymmetry and asymptote slope of the respective distributions. The blue circle represents the inflection point of the logistic distribution. γ , activity coefficient

The extensive thermodynamic potential of open, single-phase, multicomponent systems can be expressed as a Massieu-Planck function related to extensive entropy [64]. In our case this potential, which we call here lambda potential, includes molecular entropy and conformational entropy and is therefore suitable for the description of our self-organizing system (Fig. 4). Steady state is reached when

the lambda potential of the system is kept constant, quasi-equilibrium is reached when it equals that of the thermodynamic buffer. This corresponds to the equivalence of the extensive entropy potentials of the system and the reservoir. By seeking to minimize its enthalpy, the system decreases ν , increases the interaction between its components, while also seeking to maximize its entropy. As discussed above, when $1/\nu$ is equal to the golden ratio, φ , the system reaches quasi-equilibrium (Eq.(10)). The self-similarity represented by φ renders the system self-sufficient: the system “fills” reservoir, interactions between Ab and Ag fit into the binding funnels and chemical potentials of free and bound Ag are equal. Interestingly, Ab can also contribute to such a quasi-equilibrium by binding to themselves, a concept worked out by Niels Jerne, and a phenomenon observed as anti-idiotype networks [65]. In contrast to the immune network theory, our model suggests that the anti-idiotype networks are not a driving force but could rather function as a stabilizing mechanism in the system. While environmental stimuli induce dynamic responses (active immunity), networks form during the contraction phase and drive the system towards an ideal self-sufficient state (resting immunity, memory).

If we can apply statistical thermodynamics functions to a biological system it is then tempting to extend the proposed mechanism of steady states of self-organization universally. Our model suggests that the key to maintenance of the self-organizing system is the mutual interaction with a diverse environment. Therefore, we can try to seek for analogies with a generalized entropy function, such as the Rényi entropy. Rewritten from [66,67] for better comparability with Eq.(3), Rényi entropy S_q of order q is a function of energy states E_i and free energy F

$$S_q = \frac{1}{1-q} \ln \sum_i \left(\frac{1}{e^{\beta(E_i - F)}} \right)^q \quad (20)$$

Fuentes and Concalves recently proposed that “Rényi entropy automatically arises as the average rate of change of free energy over an ensemble at different temperatures” [68]. Baez expressed this as “the Rényi entropy is the the ‘ $q-1$ -derivative’ of the negative free energy”[66]. These approaches identify the order parameter of Rényi entropy as a deformation parameter that distorts the relative free energy in non-isothermal processes [67]. A similar distortion is represented by the heat capacity ratio (also called isentropic coefficient). Our approach suggests that in a self-organizing system this parameter corresponds to the distortion attributable to the hierarchy of interactions in the molecular ensemble, constituting isothermal chains of reactions.

The origin of power law behind some phenomena [69] may be attributable to the mechanism shown here when natural networks are implicated [70]. In physical terms, it arises when microscopic statistical properties of a macroscopic intensive property are examined (like gas molecule speed distribution and pressure, vibrational energies and temperature) and interactions of components cause a deformation in the distribution. The lambda potential arises from the distribution of free energy states (chemical potentials), which requires the generation of a diversity of molecule shapes. The random process of antibody gene rearrangement results in a Gaussian distribution of interaction energies, and is combined with a selection process for exponentially distributed energy in the surroundings [6,7]. In the resulting mixture of normal and exponential distributions the deformation parameter is the ratio of the standard deviations of the functions.

We can also attempt to generalize these thermodynamic concepts and merge them into the following definitions of life. “Dissipative structures are stable and self-healing in the sense that if the structure is perturbed, the processes that created it can also restore it. The processes that create the structure also “heal” the structure from damage, an important property of all living organisms. [71]” “Life is a far from equilibrium self-maintaining chemical system capable of processing, transforming and accumulating information acquired from the environment. [72]” Our model suggests that adaptive self-organization is in fact not far from equilibrium, but is the ability to maintain meta-stable equilibrium by actively arranging the system’s interaction space with the environment. Diversity in the environment is a requirement for generating diversity in the system. In our interpretation “Life of an

organism is the maintenance of steady state in a chemical energy transfer system which operates in molecular conformation space, balancing entropy and enthalpy so as to counteract changes in the surroundings.” This balancing then leads to the processing, transforming and accumulating information acquired from the environment; these processes manifest as evolution and adaptation – events that are critical beyond the functioning of the immune system. The organization of lives of organisms, a society, an ecosystem, can be possibly considered as events with a higher level of organization based on similar concepts, where the deformation parameter of thermodynamic potentials characterizes the architecture of organization.

Acknowledgments: The author wishes to thank Tamás Pfeil (Department of Applied Analysis and Computational Mathematics, Eötvös Loránd University, Budapest, Hungary) for his advices and insightful discussions on the mathematics of logistic growth.

Appendix A

Complementarity of FD and LD

$$P(\mu) = 1 - \frac{1}{1 + e^{-\beta(E-\mu)}} = \frac{e^{-\beta(E-\mu)}}{1 + e^{-\beta(E-\mu)}} = \frac{1}{1 + e^{\beta(E-\mu)}}$$

Appendix B

When parameterized for growth as a function of time, the logistic function is

$$p(t) = \frac{1}{1 + e^{-k(t-t_i)}}$$

where t_i stands for the time when growth reaches midpoint, t is time of growth and k is the rate of growth. In this case p is the probability of reaching maximal size. From this perspective growth is the probing of the environment for resources of growth. The environment, in the statistical thermodynamics interpretation, is the system, which at first has easily available (high energy) and later less accessible (low energy) resources. The growing entity probes the system for resources (energy). The size of the entity is a reflection of the resources that have been available to it and we perceive interactions between systems as time [73]. Growth is the accumulation of the constituent entities, e.g. cells of an organism, so probabilities here refer to the filling of “energy levels” by the entities. Energy levels therefore refer to the potential differences between the environment (system) and the growing organism (probe). As the number of events/entities gets very high, the stochastic process of filling energy levels becomes a deterministic process of growth.

Conflict of interest

The author declares no conflict of interest.

Data accessibility

Not applicable.

Ethics statement

Not applicable.

Funding

This research was not supported by any dedicated funding.

References

1. Sotelo, J. The nervous and the immune systems: conspicuous physiological analogies. *J. Comp. Physiol. A Neuroethol. Sens. Neural Behav. Physiol.* **2015**, *201*, 185–194, doi:10.1007/s00359-014-0961-8.
2. Grignolio, A.; Mishto, M.; Faria, A.M.C.; Garagnani, P.; Franceschi, C.; Tieri, P. Towards a liquid self: how time, geography, and life experiences reshape the biological identity. *Front. Immunol.* **2014**, *5*, 153, doi:10.3389/fimmu.2014.00153.
3. Prechl, J.; Papp, K.; Kovács, Á.; Pfeil, T. The binding landscape of serum antibodies: how physical and mathematical concepts can advance systems immunology. *Antibodies (Basel)* **2022**, *11*, 43, doi:10.3390/antib11030043.
4. Pekař, M. Thermodynamic driving forces and chemical reaction fluxes; reflections on the steady state. *Molecules* **2020**, *25*, doi:10.3390/molecules25030699.
5. Prechl, J. A generalized quantitative antibody homeostasis model: regulation of B-cell development by BCR saturation and novel insights into bone marrow function. *Clin. Transl. Immunology* **2017**, *6*, e130, doi:10.1038/cti.2016.89.
6. Prechl, J. Network organization of antibody interactions in sequence and structure space: the RADARS model. *Antibodies (Basel)* **2020**, *9*, doi:10.3390/antib9020013.
7. Prechl, J. Complex Physical Properties of an Adaptive, Self-Organizing Biological System. *Biophysica* **2023**, *3*, 231–251, doi:10.3390/biophysica3020015.
8. Hong, B.; Wu, Y.; Li, W.; Wang, X.; Wen, Y.; Jiang, S.; Dimitrov, D.S.; Ying, T. In-Depth Analysis of Human Neonatal and Adult IgM Antibody Repertoires. *Front. Immunol.* **2018**, *9*, 128, doi:10.3389/fimmu.2018.00128.
9. Galson, J.D.; Trück, J.; Fowler, A.; Münz, M.; Cerundolo, V.; Pollard, A.J.; Lunter, G.; Kelly, D.F. In-Depth Assessment of Within-Individual and Inter-Individual Variation in the B Cell Receptor Repertoire. *Front. Immunol.* **2015**, *6*, 531, doi:10.3389/fimmu.2015.00531.
10. Kono, N.; Sun, L.; Toh, H.; Shimizu, T.; Xue, H.; Numata, O.; Ato, M.; Ohnishi, K.; Itamura, S. Deciphering antigen-responding antibody repertoires by using next-generation sequencing and confirming them through antibody-gene synthesis. *Biochem. Biophys. Res. Commun.* **2017**, *487*, 300–306, doi:10.1016/j.bbrc.2017.04.054.
11. Liao, H.; Li, S.; Yu, Y.; Yue, Y.; Su, K.; Zheng, Q.; Jiang, N.; Zhang, Z. Characteristics of Plasmablast Repertoire in Chronically HIV-Infected Individuals for Immunoglobulin H and L Chain Profiled by Single-Cell Analysis. *Front. Immunol.* **2019**, *10*, 3163, doi:10.3389/fimmu.2019.03163.
12. Miyasaka, A.; Yoshida, Y.; Wang, T.; Takikawa, Y. Next-generation sequencing analysis of the human T-cell and B-cell receptor repertoire diversity before and after hepatitis B vaccination. *Hum. Vaccin. Immunother.* **2019**, doi:10.1080/21645515.2019.1600987.

13. IJspeert, H.; van Schouwenburg, P.A.; van Zessen, D.; Pico-Knijnenburg, I.; Driessen, G.J.; Stubbs, A.P.; van der Burg, M. Evaluation of the Antigen-Experienced B-Cell Receptor Repertoire in Healthy Children and Adults. *Front. Immunol.* **2016**, *7*, 410, doi:10.3389/fimmu.2016.00410.
14. Csepregi, L.; Hoehn, K.B.; Neumeier, D.; Taft, J.M.; Friedensohn, S.; Weber, C.R.; Kummer, A.; Sesterhenn, F.; Correia, B.E.; Reddy, S.T. The physiological landscape and specificity of antibody repertoires. *BioRxiv* **2021**, doi:10.1101/2021.09.15.460420.
15. Miho, E.; Roškar, R.; Greiff, V.; Reddy, S.T. Large-scale network analysis reveals the sequence space architecture of antibody repertoires. *Nat. Commun.* **2019**, *10*, 1321, doi:10.1038/s41467-019-09278-8.
16. Weber, C.R.; Rubio, T.; Wang, L.; Zhang, W.; Robert, P.A.; Akbar, R.; Snapkov, I.; Wu, J.; Kuijjer, M.L.; Tarazona, S.; Conesa, A.; Sandve, G.K.; Liu, X.; Reddy, S.T.; Greiff, V. Reference-based comparison of adaptive immune receptor repertoires. *Cell Rep. Methods* **2022**, *2*, 100269, doi:10.1016/j.crmeth.2022.100269.
17. Christley, S.; Scarborough, W.; Salinas, E.; Rounds, W.H.; Toby, I.T.; Fonner, J.M.; Levin, M.K.; Kim, M.; Mock, S.A.; Jordan, C.; Ostmeyer, J.; Buntzman, A.; Rubelt, F.; Davila, M.L.; Monson, N.L.; Scheuermann, R.H.; Cowell, L.G. VDJServer: A Cloud-Based Analysis Portal and Data Commons for Immune Repertoire Sequences and Rearrangements. *Front. Immunol.* **2018**, *9*, 976, doi:10.3389/fimmu.2018.00976.
18. Sevy, A.M.; Soto, C.; Bombardi, R.G.; Meiler, J.; Crowe, J.E. Immune repertoire fingerprinting by principal component analysis reveals shared features in subject groups with common exposures. *BMC Bioinformatics* **2019**, *20*, 629, doi:10.1186/s12859-019-3281-8.
19. Chardès, V.; Vergassola, M.; Walczak, A.M.; Mora, T. Affinity maturation for an optimal balance between long-term immune coverage and short-term resource constraints. *Proc Natl Acad Sci USA* **2022**, *119*, doi:10.1073/pnas.2113512119.
20. Mora, T.; Walczak, A.M.; Bialek, W.; Callan, C.G. Maximum entropy models for antibody diversity. *Proc Natl Acad Sci USA* **2010**, *107*, 5405–5410, doi:10.1073/pnas.1001705107.
21. Bryngelson, J.D.; Wolynes, P.G. Spin glasses and the statistical mechanics of protein folding. *Proc Natl Acad Sci USA* **1987**, *84*, 7524–7528, doi:10.1073/pnas.84.21.7524.
22. Bryngelson, J.D.; Onuchic, J.N.; Soccia, N.D.; Wolynes, P.G. Funnels, pathways, and the energy landscape of protein folding: a synthesis. *Proteins* **1995**, *21*, 167–195, doi:10.1002/prot.340210302.
23. Ma, B.; Kumar, S.; Tsai, C.J.; Nussinov, R. Folding funnels and binding mechanisms. *Protein Eng.* **1999**, *12*, 713–720, doi:10.1093/protein/12.9.713.
24. Wang, J.; Oliveira, R.J.; Chu, X.; Whitford, P.C.; Chahine, J.; Han, W.; Wang, E.; Onuchic, J.N.; Leite, V.B.P. Topography of funneled landscapes determines the thermodynamics and kinetics of protein folding. *Proc Natl Acad Sci USA* **2012**, *109*, 15763–15768, doi:10.1073/pnas.1212842109.
25. Wolynes, P.G. Evolution, energy landscapes and the paradoxes of protein folding. *Biochimie* **2015**, *119*, 218–230, doi:10.1016/j.biochi.2014.12.007.
26. Finkelstein, A.V.; Badretdin, A.J.; Galzitskaya, O.V.; Ivankov, D.N.; Bogatyreva, N.S.; Garbuzynskiy, S.O. There and back again: Two views on the protein folding puzzle. *Phys. Life Rev.* **2017**, *21*, 56–71, doi:10.1016/j.plrev.2017.01.025.

27. Yan, Z.; Wang, J. Funneled energy landscape unifies principles of protein binding and evolution. *Proc Natl Acad Sci USA* **2020**, *117*, 27218–27223, doi:10.1073/pnas.2013822117.

28. Onuchic, J.N.; Luthey-Schulten, Z.; Wolynes, P.G. Theory of protein folding: the energy landscape perspective. *Annu. Rev. Phys. Chem.* **1997**, *48*, 545–600, doi:10.1146/annurev.physchem.48.1.545.

29. Schug, A.; Onuchic, J.N. From protein folding to protein function and biomolecular binding by energy landscape theory. *Curr. Opin. Pharmacol.* **2010**, *10*, 709–714, doi:10.1016/j.coph.2010.09.012.

30. Boehr, D.D.; Nussinov, R.; Wright, P.E. The role of dynamic conformational ensembles in biomolecular recognition. *Nat. Chem. Biol.* **2009**, *5*, 789–796, doi:10.1038/ncembio.232.

31. Abdelsattar, A.S.; Mansour, Y.; Aboul-Ela, F. The Perturbed Free-Energy Landscape: Linking Ligand Binding to Biomolecular Folding. *Chembiochem* **2021**, *22*, 1499–1516, doi:10.1002/cbic.202000695.

32. Foote, J.; Milstein, C. Conformational isomerism and the diversity of antibodies. *Proc Natl Acad Sci USA* **1994**, *91*, 10370–10374, doi:10.1073/pnas.91.22.10370.

33. Thielges, M.C.; Zimmermann, J.; Yu, W.; Oda, M.; Romesberg, F.E. Exploring the energy landscape of antibody-antigen complexes: protein dynamics, flexibility, and molecular recognition. *Biochemistry* **2008**, *47*, 7237–7247, doi:10.1021/bi800374q.

34. Wedemayer, G.J.; Patten, P.A.; Wang, L.H.; Schultz, P.G.; Stevens, R.C. Structural insights into the evolution of an antibody combining site. *Science* **1997**, *276*, 1665–1669, doi:10.1126/science.276.5319.1665.

35. Fernández-Quintero, M.L.; Loeffler, J.R.; Kraml, J.; Kahler, U.; Kamenik, A.S.; Liedl, K.R. Characterizing the Diversity of the CDR-H3 Loop Conformational Ensembles in Relationship to Antibody Binding Properties. *Front. Immunol.* **2018**, *9*, 3065, doi:10.3389/fimmu.2018.03065.

36. Fernández-Quintero, M.L.; Georges, G.; Varga, J.M.; Liedl, K.R. Ensembles in solution as a new paradigm for antibody structure prediction and design. *MAbs* **2021**, *13*, 1923122, doi:10.1080/19420862.2021.1923122.

37. Shmool, T.A.; Martin, L.K.; Bui-Le, L.; Moya-Ramirez, I.; Kotidis, P.; Matthews, R.P.; Venter, G.A.; Kontoravdi, C.; Polizzi, K.M.; Hallett, J.P. An experimental approach probing the conformational transitions and energy landscape of antibodies: a glimmer of hope for reviving lost therapeutic candidates using ionic liquid. *Chem. Sci.* **2021**, *12*, 9528–9545, doi:10.1039/dlsc02520a.

38. Phillips, A.M.; Lawrence, K.R.; Moulana, A.; Dupic, T.; Chang, J.; Johnson, M.S.; Cvijovic, I.; Mora, T.; Walczak, A.M.; Desai, M.M. Binding affinity landscapes constrain the evolution of broadly neutralizing anti-influenza antibodies. *eLife* **2021**, *10*, doi:10.7554/eLife.71393.

39. Smith, D.J.; Lapedes, A.S.; de Jong, J.C.; Bestebroer, T.M.; Rimmelzwaan, G.F.; Osterhaus, A.D.M.E.; Fouchier, R.A.M. Mapping the antigenic and genetic evolution of influenza virus. *Science* **2004**, *305*, 371–376, doi:10.1126/science.1097211.

40. Fonville, J.M.; Wilks, S.H.; James, S.L.; Fox, A.; Ventresca, M.; Aban, M.; Xue, L.; Jones, T.C.; Le, N.M.H.; Pham, Q.T.; Tran, N.D.; Wong, Y.; Mosterin, A.; Katzelnick, L.C.; Labonte, D.; Le, T.T.; van der Net, G.; Skepner, E.; Russell, C.A.; Kaplan, T.D.; Rimmelzwaan, G.F.; Masurel, N.; de Jong, J.C.; Palache, A.; Beyer, W.E.P.; Le, Q.M.; Nguyen, T.H.; Wertheim, H.F.L.; Hurt, A.C.; Osterhaus, A.D.M.E.; Barr, I.G.; Fouchier, R.A.M.; Horby, P.W.; Smith,

D.J. Antibody landscapes after influenza virus infection or vaccination. *Science* **2014**, *346*, 996–1000, doi:10.1126/science.1256427.

41. Shortle, D.; Chan, H.S.; Dill, K.A. Modeling the effects of mutations on the denatured states of proteins. *Protein Sci.* **1992**, *1*, 201–215, doi:10.1002/pro.5560010202.

42. Bornberg-Bauer, E.; Chan, H.S. Modeling evolutionary landscapes: mutational stability, topology, and superfunnels in sequence space. *Proc Natl Acad Sci USA* **1999**, *96*, 10689–10694, doi:10.1073/pnas.96.19.10689.

43. Desponts, J.; Mora, T.; Walczak, A.M. Fluctuating fitness shapes the clone-size distribution of immune repertoires. *Proc Natl Acad Sci USA* **2016**, *113*, 274–279, doi:10.1073/pnas.1512977112.

44. de Greef, P.C.; Oakes, T.; Gerritsen, B.; Ismail, M.; Heather, J.M.; HermSEN, R.; Chain, B.; de Boer, R.J. The naive T-cell receptor repertoire has an extremely broad distribution of clone sizes. *eLife* **2020**, *9*, doi:10.7554/eLife.49900.

45. Reed, W.J.; Hughes, B.D. From gene families and genera to incomes and internet file sizes: why power laws are so common in nature. *Phys. Rev. E Stat. Nonlin. Soft Matter Phys.* **2002**, *66*, 067103, doi:10.1103/PhysRevE.66.067103.

46. Tél, T. Fractals, multifractals, and thermodynamics. *Z.Naturforsch.* **1988**, *43a*, 1154–1174.

47. Zmeskal, O.; Dzik, P.; Vesely, M. Entropy of fractal systems. *Computers & Mathematics with Applications* **2013**, *66*, 135–146, doi:10.1016/j.camwa.2013.01.017.

48. Song, C.; Havlin, S.; Makse, H.A. Self-similarity of complex networks. *Nature* **2005**, *433*, 392–395, doi:10.1038/nature03248.

49. Song, C.; Havlin, S.; Makse, H.A. Origins of fractality in the growth of complex networks. *Nat. Phys.* **2006**, *2*, 275–281, doi:10.1038/nphys266.

50. Gottschalk, P.G.; Dunn, J.R. The five-parameter logistic: a characterization and comparison with the four-parameter logistic. *Anal. Biochem.* **2005**, *343*, 54–65, doi:10.1016/j.ab.2005.04.035.

51. Cumberland, W.N.; Fong, Y.; Yu, X.; Defawe, O.; Frahm, N.; De Rosa, S. Nonlinear Calibration Model Choice between the Four and Five-Parameter Logistic Models. *J. Biopharm. Stat.* **2015**, *25*, 972–983, doi:10.1080/10543406.2014.920345.

52. Goutelle, S.; Maurin, M.; Rougier, F.; Barbaut, X.; Bourguignon, L.; Ducher, M.; Maire, P. The Hill equation: a review of its capabilities in pharmacological modelling. *Fundam. Clin. Pharmacol.* **2008**, *22*, 633–648, doi:10.1111/j.1472-8206.2008.00633.x.

53. Buchwald, P. A single unified model for fitting simple to complex receptor response data. *Sci. Rep.* **2020**, *10*, 13386, doi:10.1038/s41598-020-70220-w.

54. Gesztelyi, R.; Zsuga, J.; Kemeny-Beke, A.; Varga, B.; Juhasz, B.; Tosaki, A. The Hill equation and the origin of quantitative pharmacology. *Arch. Hist. Exact Sci.* **2012**, *66*, 427–438, doi:10.1007/s00407-012-0098-5.

55. Islam, M.A.; Chowdhury, M.A.; Mozumder, M.S.I.; Uddin, M.T. Langmuir adsorption kinetics in liquid media: interface reaction model. *ACS Omega* **2021**, *6*, 14481–14492, doi:10.1021/acsomega.1c01449.

56. Kim, S.-C.; Arun, A.S.; Ahsen, M.E.; Vogel, R.; Stolovitzky, G. The Fermi-Dirac distribution provides a calibrated probabilistic output for binary classifiers. *Proc Natl Acad Sci USA* **2021**, *118*, doi:10.1073/pnas.2100761118.

57. Tsoularis, A.; Wallace, J. Analysis of logistic growth models. *Math. Biosci.* **2002**, *179*, 21–55, doi:10.1016/S0025-5564(02)00096-2.

58. Ekins, R.; Chu, F.; Biggart, E. Multispot, multianalyte, immunoassay. *Ann Biol Clin (Paris)* **1990**, *48*, 655–666.

59. Saviranta, P.; Okon, R.; Brinker, A.; Warashina, M.; Eppinger, J.; Geierstanger, B.H. Evaluating sandwich immunoassays in microarray format in terms of the ambient analyte regime. *Clin. Chem.* **2004**, *50*, 1907–1920, doi:10.1373/clinchem.2004.037929.

60. Papp, K.; Kovács, Á.; Orosz, A.; Hérincs, Z.; Randek, J.; Liliom, K.; Pfeil, T.; Prechl, J. Absolute Quantitation of Serum Antibody Reactivity Using the Richards Growth Model for Antigen Microspot Titration. *Sensors* **2022**.

61. Richards, F.J. A flexible growth function for empirical use. *J. Exp. Bot.* **1959**, *10*, 290–301, doi:10.1093/jxb/10.2.290.

62. Fong, Y.; Wakefield, J.; De Rosa, S.; Frahm, N. A robust bayesian random effects model for nonlinear calibration problems. *Biometrics* **2012**, *68*, 1103–1112, doi:10.1111/j.1541-0420.2012.01762.x.

63. Kovacs, A.; Herincs, Z.; Papp, K.; Kaczmarek, J.Z.; Larsen, D.N.; Stage, P.; Bereczki, L.; Ujhelyi, E.; Pfeil, T.; Prechl, J. Deep physico-chemical characterization of individual serum antibody responses against SARS-CoV-2 RBD using a dual titration microspot assay. *BioRxiv* **2023**, doi:10.1101/2023.03.14.532012.

64. Wilhelm, E. CHAPTER 1. gibbs energy and helmholtz energy: introduction, concepts and selected applications. In *Gibbs energy and helmholtz energy: liquids, solutions and vapours*; Wilhelm, E., Letcher, T. M., Eds.; Royal Society of Chemistry: Cambridge, 2021; pp. 1–120 ISBN 978-1-83916-201-5.

65. Jerne, N.K. Towards a network theory of the immune system. *Ann Immunol (Paris)* **1974**, *125C*, 373–389.

66. Baez, J.C. Rényi entropy and free energy. *Entropy (Basel)* **2022**, *24*, doi:10.3390/e24050706.

67. Mora, T.; Walczak, A.M. Rényi entropy, abundance distribution, and the equivalence of ensembles. *Phys. Rev. E* **2016**, *93*, 052418, doi:10.1103/PhysRevE.93.052418.

68. Fuentes, J.; Gonçalves, J. Rényi entropy in statistical mechanics. *Entropy (Basel)* **2022**, *24*, doi:10.3390/e24081080.

69. Newman, M.E.J. Power laws, Pareto distributions and Zipf's law. *Contemp. Phys.* **2005**, *46*, 323–351, doi:10.1080/00107510500052444.

70. Hartonen, T.; Annila, A. Natural networks as thermodynamic systems. *Complexity* **2012**, *18*, 53–62, doi:10.1002/cplx.21428.

71. Chung, B.J.; De Bari, B.; Dixon, J.; Kondepudi, D.; Pateras, J.; Vaidya, A. On the Thermodynamics of Self-Organization in Dissipative Systems: Reflections on the Unification of Physics and Biology. *Fluids* **2022**, *7*, 141, doi:10.3390/fluids7040141.

72. Vitas, M.; Dobovišek, A. Towards a general definition of life. *Orig. Life Evol. Biosph.* **2019**, *49*, 77–88, doi:10.1007/s11084-019-09578-5.
73. Lucia, U.; Grisolia, G. Thermodynamic definition of time: considerations on the EPR paradox. *Mathematics* **2022**, *10*, 2711, doi:10.3390/math10152711.